Technical Paper

ISSN 1997-1400 Int. J. Pavement Res. Technol. 4(6):337-346

Finite Element Analysis of Instrumented Thin Flexible Pavement to Quantify Variability

Isaac L. Howard[1+] and Kimberly A. Warren[2]

Abstract: Variability analysis is used for an instrumented pavement consisting of a thin asphalt surface, granular base, geosynthetics, and a fine grained subgrade. The pavement was modeled with the finite element method using Plaxis software where stationary transient loading and stress dependent material models were incorporated. The results show how significant variability can occur within a pavement built to acceptable standards and that without methods to account for variability, instrumented measurements can be misleading in some instances. Realizing that variability is present is far removed from accounting for it effectively. Asphalt strain changes from 8% to 141% were calculated due to the effects of variability, and vertical sensor positioning within customary installation tolerances was shown to vary strain by ± 31%. The use of asphalt strain gauges in thin flexible pavements was shown to be highly prone to error, with variability easily dominating the measurement. Subgrade stress changes from 17% to 45% were calculated from the effects of variability, and vertical sensor positioning with customary installation tolerances was shown to vary pressure by ±3%. Subgrade stress variability was less relative to asphalt strain, though it was too high to neglect in analysis.

***Key words**: Finite Element Method; Instrumentation; Thin Flexible Pavement; Variability.*

Introduction

Full scale instrumented pavements have gained favor in the United States in recent years. Notable examples have been performed in Alabama [1], Arkansas [2], Minnesota [3], Ohio [4], Pennsylvania [5], and Virginia [6]. They are either constructed within in service pavements, such as those managed by Departments of Transportation (DOTs), or within controlled test facilities. The need to account for variability in pavements has been understood since the *AASHO Road Test*. Of more significance in the present day is the effective handling of variability in such a way to achieve meaningful conclusions. Quantifiable variability information related to instrumented pavements, especially thin flexible pavements, is not well established in literature.

Agency construction specifications allow for layer thickness variability that, while acceptable to the agency, should be considered when planning for and/or analyzing data from in-situ instrumented test sections, in particular with thin test sections. The *Mississippi Department of Transportation* [7] has an asphalt thickness tolerance of approximately ±1 cm with the (-) requiring overlay of the pavement and the (+) requiring price adjustments. The majority of cases in [7] have a ±2.5 cm base course thickness tolerance. The *Arkansas Highway and Transportation Department* (AHTD) specifies rates of asphalt application on their plans. Typically 60 kg/m^2 is the equivalent of 2.54 cm of asphalt. The actual rate applied does not fall under pavement acceptance, and personal communication with AHTD engineers revealed the latitude of the Resident Engineer to exceed the plan quantity by 10%.

Layer thickness variability is also present in test facilities. *As built* asphalt thicknesses ranging from 9.7 cm to 11.2 cm were reported by Prowell [8] for an *as designed* thickness of 10.2 cm in the 2000 construction cycle of the National Center for Asphalt Technology (NCAT) test track. Overall, the forty-six section test track had an average constructed asphalt thickness of 10.4 cm, a section standard deviation of approximately 0.25 cm, and a coefficient of variation (*cov*) of 2.4%.

Material property variability is also a notable contributor to the total variability within a pavement. Darter *et al.* [9] performed in-situ dynamic load tests that produced stiffness terms with a *cov* of 14% to 17% for the thinnest pavements investigated. AASHTO [10] reported *cov* values of 10% and 14% for the strength factor terms representing the asphalt and granular base, respectively. A literature review performed by Freeman and Grogram [11] reported the properties of multiple pavement materials. Coefficients of variation were reported to be 10% for the granular base unconfined compressive strength and angle of internal friction, while coefficients of variation were reported to be 9% to 23% for the dynamic modulus of highway quality asphalt concrete.

The primary objective of this paper is to utilize finite element analysis to quantify the variability of thin flexible pavements as it relates to performance prediction. Layer thickness variability is investigated in absence of pavement material variability. Subsequently, layer thickness variability is analyzed in conjunction with pavement material variability. The authors could not locate an analysis of this nature in the literature.

The effects of vertical position tolerances, in-place misalignment, imperfect calibration, and/or alteration of the stress field lead to measurement variability. A limited and mixed set of approaches have been used to evaluate measurement variability, with most approaches relying heavily on measured data. According to Brown [12], accuracies better than ±20% cannot be expected for a pressure measurement because of the many difficulties involved (i.e. stress cannot be measured directly and must rely on strain or deformation

[1] Civil and Environmental Engineering, Mississippi State University, 501 Hardy Road, Mississippi State, MS 39762, USA.
[2] Civil and Environmental Engineering, UNC Charlotte, 9201 University City Boulevard, Charlotte, NC 28223-0001, USA.
[+] Corresponding Author: E-mail ilhoward@cee.msstate.edu
Note: Submitted November 15, 2010; Revised March 29, 2011; Accepted April 12, 2011.

within the instrument). Tabatabaee *et al.* [5] evaluated the performance of asphalt strain gauges and earth pressure cells and found the *cov* for the instruments to be up to 6% for asphalt strain measurements and less than 10% for earth pressure measurements. Siddharthan *et al.* [13] tested two pavements (7.6 cm HMA over 30 cm aggregate base was the smaller of the two) and reported a *cov* of less than 5% for replicate pressure measurements, noting that strain differences of ±30% should be expected. Willis and Timm [14] collected 80,000 asphalt strain readings from paired gauges. Approximately 80% of the strain readings were within 30 με, and nearly 100% of the strain readings were within 100 με.

Analytical techniques have also been used to investigate measurement variability. As an example, Zafar *et al.* [15] performed finite element analysis of high stiffness pressure cells embedded in asphalt concrete. The analysis revealed potential errors due to stress field alterations and concluded that a method to calculate the error and remove it from the readings was needed. In addition to the analytical knowledge base, the secondary objective of this paper is to use finite element analysis to investigate the effect vertical installation tolerances of instrumentation can have on thin flexible pavement's predicted performance.

The usefulness of the information presented in this paper lies in allowing more informed planning of and/or analyzing data from instrumented test sections, especially with thin sections. The goal of test sections such as those considered in this paper is to measure the performance effect of a given variable (e.g. geosynthetics). To achieve this goal, test sections must be as uniform as possible, and any variability associated with non-uniformity must be addressed during analysis. For example, to detect contamination and stiffness reduction of base materials due to subgrade intrusion noted to be problematic by Jorenby and Hicks [16] and assess its effect on pavement performance, measured results must be analyzed so that the portion of the measurement due to contamination is isolated. Another example is that Brunton and Akroyde [17] studied sixteen instrumented test sections containing geogrids and geotextiles over a four year period in the presence of truck traffic and FWD testing and produced no specific conclusions related to the geosynthetics. Coring of the pavement showed some layer thicknesses were outside specification, while FWD testing showed thickness and pavement material variability were evident along sections that had the same nominal properties. Brunton and Akroyde [17] emphasized the importance of accurate layer thicknesses at the points analyzed, and the study resulted in several generalizations that appeared to be due, at least in part, to variability.

Pavement Modeled

Most of the data used to develop the thin flexible pavement modeled in this paper has already been presented in Arkansas [2]. Table 1 shows the *as built* properties that were measured during construction and testing. The values are in line with the Arkansas and Mississippi DOT construction specifications presented previously, and since layer thicknesses and subgrade moduli were measured sixteen times within the pavement, it was considered suitable for variability analysis. Additionally, the pavement contained two thin flexible designs. Geosynthetics were installed at the surface of the subgrade in all but two of the sixteen test sections.

Table 1. As Built Properties of Pavement Modeled

Design	Section[1]	Thickness (cm)		M_r (MPa)
		HMA	Base	Subgrade
1	Maximum	6.2	29.4	84
	Minimum	5.7	23.3	67
	Average	5.9	24.6	72
	Designed	5.1	25.4	---
2	Maximum	6.5	16.8	87
	Minimum	5.6	14.1	76
	Average	6.0	15.9	83
	Designed	5.1	15.2	---

1: Values indicate the maximum, minimum, and average measured properties of the eight sections that were built according to Design 1 or Design 2. The design refers to the layer thickness on construction plans.

The hot mixed asphalt (HMA) was a 12.5 mm Superpave mix, the binder grade was PG 64-22, and the layer thicknesses were determined from the asphalt cores collected. The base was a crushed limestone with a dry density of 22.5 kN/m^3, an apparent specific gravity of 2.80, and an internal friction angle of 43°. The base course thicknesses were determined via surveying. Modulus variability of the HMA and base course was not measured during testing. When pavement material variability was simulated in the finite element model, a plausible range was estimated based on the literature review provided in the previous section.

The subgrade was classified as a fat clay (CH) with a plasticity index ranging from 35 to 54. Subgrade resilient modulus (M_r) values were back calculated from Falling Weight Deflectometer (FWD) test data acquired during each test phase using the approach of Hall and Elliott [18]. For the duration considered, average M_r values ranged from 63 MPa to 87 MPa corresponding to a period where subgrade moisture contents were near optimum conditions. Soil samples taken during construction were tested in accordance with AASHTO T 307 protocol near an optimum moisture with a 13.8 kPa confining pressure and deviator stress in excess of 40 kPa, which resulted in laboratory M_r values of 79 MPa to 89 MPa. The subgrade conditions were consistent during the period used for testing, which meant that only asphalt temperature had to be considered in the assessment, reducing the number of calculations required.

Thirty-one cases were modeled and are shown in Table 2. For each pavement design, case A used average layer thicknesses, case B used *as designed* layer thicknesses, cases C and D used the highest layer thickness, and cases E and F used the lowest layer thickness. Cases A through F used anticipated asphalt and limestone base moduli. Cases G through L varied asphalt and limestone base moduli by thirty percent relative to the anticipated condition and considered as designed, highest, and lowest layer thicknesses. Cases I through L were selected to represent the extreme soil modulus and layer thickness combinations that could occur due to variability and were measured in the test sections. This selection was aided by finite element modeling not shown in the paper. Cases M through P were modeled with fifteen percent variability in asphalt and limestone base moduli. The conditions modeled had properties on the outer bound of cases G to L to conserve modeling effort (i.e.

Table 2. Pavement Cases Modeled

Case	Thickness (cm)		Modulus (MPa)		
	HMA	Base	E^*	E^{Ref}	M_r
1-A	5.9	24.6	5.85(10^3)	105.5	72
1-B	5.1	25.4	5.85(10^3)	105.5	72
1-C	6.2	29.4	5.85(10^3)	105.5	84
1-D	6.2	29.4	5.85(10^3)	105.5	63
1-E	5.7	22.3	5.85(10^3)	105.5	84
1-F	5.7	22.3	5.85(10^3)	105.5	63
1-G	5.1	25.4	7.61(10^3)	137.2	72
1-H	5.1	25.4	4.10(10^3)	73.9	72
1-I	6.2	29.4	7.61(10^3)	137.2	63
1-J	6.2	29.4	4.10(10^3)	73.9	63
1-K	5.7	22.3	7.61(10^3)	137.2	84
1-L	5.7	22.3	4.10(10^3)	73.9	84
1-M	5.1	25.4	6.73(10^3)	121.3	72
1-N	6.2	29.4	4.97(10^3)	89.7	63
1-O	5.7	22.3	6.73(10^3)	121.3	84
2-A	6.0	15.9	5.85(10^3)	105.5	83
2-B	5.1	15.2	5.85(10^3)	105.5	83
2-C	6.5	16.8	5.85(10^3)	105.5	87
2-D	6.5	16.8	5.85(10^3)	105.5	76
2-E	5.6	14.1	5.85(10^3)	105.5	87
2-F	5.6	14.1	5.85(10^3)	105.5	76
2-G	5.1	15.2	7.61(10^3)	137.2	83
2-H	5.1	15.2	4.10(10^3)	73.9	83
2-I	6.5	16.8	7.61(10^3)	137.2	76
2-J	6.5	16.8	4.10(10^3)	73.9	76
2-K	5.6	14.1	7.61(10^3)	137.2	87
2-L	5.6	14.1	4.10(10^3)	73.9	87
2-M	5.1	15.2	6.73(10^3)	121.3	83
2-N	5.1	15.2	4.97(10^3)	89.7	83
2-O	6.5	16.8	6.73(10^3)	121.3	76
2-P	6.5	16.8	4.97(10^3)	89.7	76

Note: p^{Ref} was 13.8 kPa for all calculations.
Note: E^* shown was at 21°C and 17 Hz.

cases G to L were performed and used to minimize cases that needed to simulate 15% material variability).

All thirty-one cases were loaded to the legal limit for many US pavements (45 kN wheel load). Each scenario was modeled as a function of asphalt temperature (≈ 0°C to 50°C) by adjusting the asphalt dynamic modulus (E^*). Nineteen simulations were performed for each case labeled A to L (456 simulations), and six simulations were performed for each case labeled M to P (42 simulations).

Finite Element Model

The finite element model developed by Howard and Warren [19] using Plaxis software [20] was used for the analysis. The axis-symmetric model applies a stationary transient load to the pavement and uses project specific inputs measured either in the laboratory or from full-scale test sections. The model has shown reasonable agreement to measured responses during full-scale trafficking. These measured responses were collected from asphalt strain gauges oriented parallel to traffic flow near the bottom of the layer, hydraulic total earth pressure cells installed at the top of the subgrade, foil strain gauges attached to the geosynthetics installed at the subgrade/base interface, and thermocouples embedded in the bottom of the asphalt layer. Only a summary of the model is provided in this paper as full details of the model are published in Howard and Warren [19].

The asphalt was modeled as linear-elastic, with E^* determined by using the *Level 2* procedure of the Mechanistic-Empirical Pavement Design Guide (MEPDG) from *NCHRP 1-37A*. The approach considers mixture properties, temperature, and rate of loading when determining E^* for use within the model, as they can have a considerable effect on strain. The geosynthetics were modeled as tension elements.

The limestone base was modeled as a hyperbolic, bulk stress hardening material. For a given material and conditions, the relationship between the reference modulus (E^{Ref}) and the reference pressure (p^{Ref}) governs model behavior. The equations relating these parameters are found in the Plaxis library and are referred to as the HS model. To establish the reference pressure, conditions measured during FWD testing were used, as shown in Eq. (1).

$$p^{Ref} = \sigma_d k_0 \tag{1}$$

σ_d is the measured deviator stress at depth of interest under FWD loading, k_o = 1-$sin\phi$, and ϕ is the Mohr-Coulomb friction angle. To establish the bulk stress hardening behavior, material from the same limestone quarry was tested in the laboratory and used to develop Eq. (2).

$$E^{Ref} = 4.57\,(3k_o\sigma_d + \sigma_d)^{0.7081} \tag{2}$$

The subgrade was modeled as a hyperbolic, deviator stress softening material. The HS model in the Plaxis library was used to assess the hyperbolic behavior alongside back calculated subgrade resilient modulus values that were used as E^{Ref} to account for deviator stress softening. The reference pressure was determined with Eq. (1). The natural ground below the subgrade was modeled with a Mohr-Coulomb approach, with inputs measured using AASHTO T 307 protocol.

Stresses and strains were calculated where the instrumentation would actually be located for a given condition rather than at a fixed (i.e. Cartesian) coordinate. Performing the calculations in this manner makes the objective of quantifying variability of instrumented pavements more tangible. Layer thickness variability is not considered in sensor positioning. Earth pressure cells are typically installed after the subgrade is constructed by excavating to a fixed depth (e.g. 19 mm) below the surface of the layer. Asphalt strain gauges are typically installed just before the layer is constructed by placing a given thickness of asphalt (e.g. 13 mm) below the gauge.

Asphalt Strain Calculation Results

Results of the FEA simulations for horizontal tensile strain in the asphalt with 0% and 30% pavement material variability are plotted

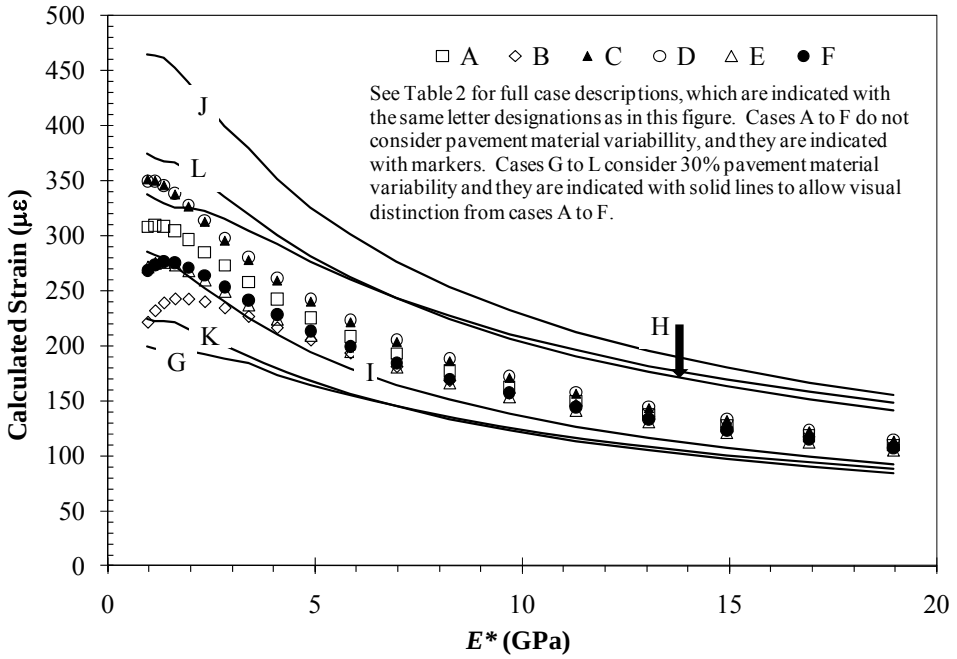

Fig. 1. Finite Element Analysis Results for Design 1 Asphalt Strain.

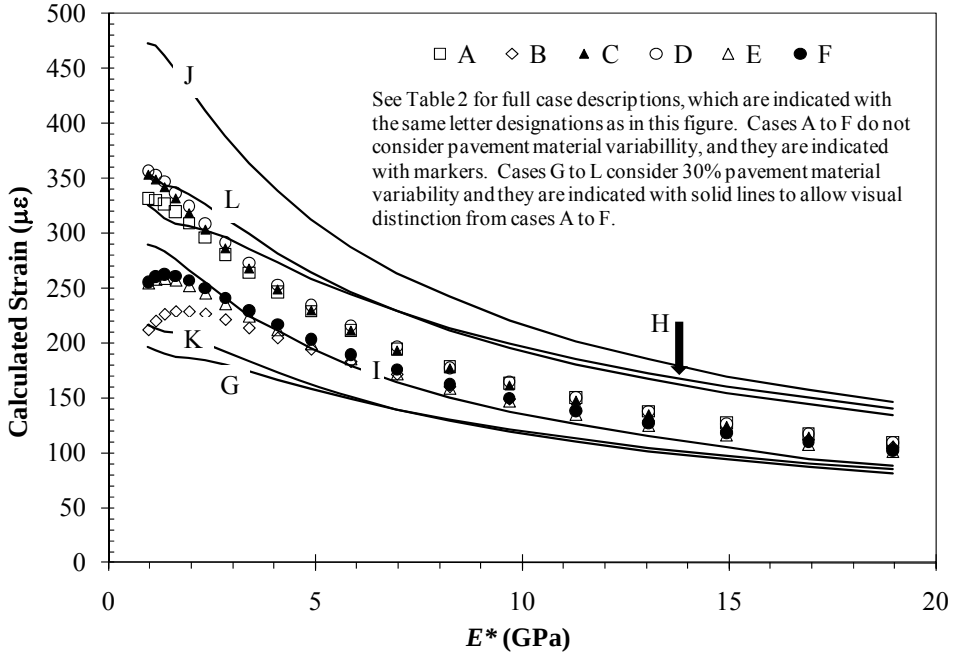

Fig. 2. Finite Element Analysis Results for Design 2 Asphalt Strain

in Figs. 1 and 2 versus anticipated asphalt modulus. The results show the asphalt strain increasing in layers ranging from 5.1 cm to 6.5 cm thick. Initially this seems counter intuitive, but it has been observed by other researchers. Huang [21] provides data showing tensile strains increasing until the asphalt thickness reached 7 cm, and thereafter, the tensile strain decreased. Asphalt strain is driven more by E^* variations than other variables, especially at high temperatures where E^* is low. Low E^* values produced high strains, and vice versa. Thicker asphalt with low modulus was the condition that produced the highest strain, and inadequate compaction would lead to this combination. Modulus was more significant than asphalt thickness, evidenced by comparing cases A and B for thickness influence and cases I and J for modulus influence (Fig. 1). When using E^*, the strain increased approximately 25% when the thickness increased 0.8 cm. In comparison, a change in modulus from 30% above typical to 30% below typical increased strain 60% at maximum thickness (defined in Table 1).

Also observable from Figs. 1 and 2 is the amount of strain variability that can occur in a full scale pavement over a short duration. The length of the pavement for this study was only 260 m.

Table 3. Asphalt Strain and Fatigue Damage Test Results

Design	Cases	E^* (GPa)	Minimum			Maximum			Percent Change	
			ε_t (με)	N_f	D_f (%)	ε_t (με)	N_f	D_f(%)	D_f(%)	ε_t (%)
1	A to F	0.96	221	600274	0.17	349	133446	0.75	0.58	58
		1.94	242	243349	0.41	328	89459	1.12	0.71	36
		4.89	204	194049	0.52	242	110603	0.90	0.39	19
		9.69	153	279218	0.36	172	189950	0.53	0.17	13
		14.93	121	417619	0.24	133	305936	0.33	0.09	10
		18.96	105	543194	0.18	115	402654	0.25	0.06	10
2	A to F	0.96	212	688293	0.15	353	128534	0.78	0.63	67
		1.94	228	296076	0.34	324	93146	1.07	0.74	42
		4.89	199	210562	0.47	234	123542	0.81	0.33	18
		9.69	147	318509	0.31	165	217783	0.46	0.15	12
		14.93	116	479839	0.21	126	365517	0.27	0.07	9
		18.96	101	617259	0.16	109	480306	0.21	0.05	8
1	G to L	0.96	199	847655	0.12	464	52268	1.91	1.80	133
		1.94	195	495293	0.20	439	34278	2.92	2.72	125
		4.89	164	397973	0.25	326	41486	2.41	2.16	99
		9.69	125	543041	0.18	232	70948	1.41	1.23	86
		14.93	100	782036	0.13	180	113012	0.88	0.76	80
		18.96	88	971396	0.10	155	150767	0.66	0.56	76
2	G to L	0.96	196	891107	0.11	473	49066	2.04	1.93	141
		1.94	186	578628	0.17	432	36140	2.77	2.59	132
		4.89	158	449908	0.22	312	47934	2.09	1.86	98
		9.69	121	604389	0.17	220	84499	1.18	1.02	82
		14.93	97	864492	0.12	170	136402	0.73	0.62	75
		18.96	85	1088858	0.09	146	183571	0.54	0.45	72

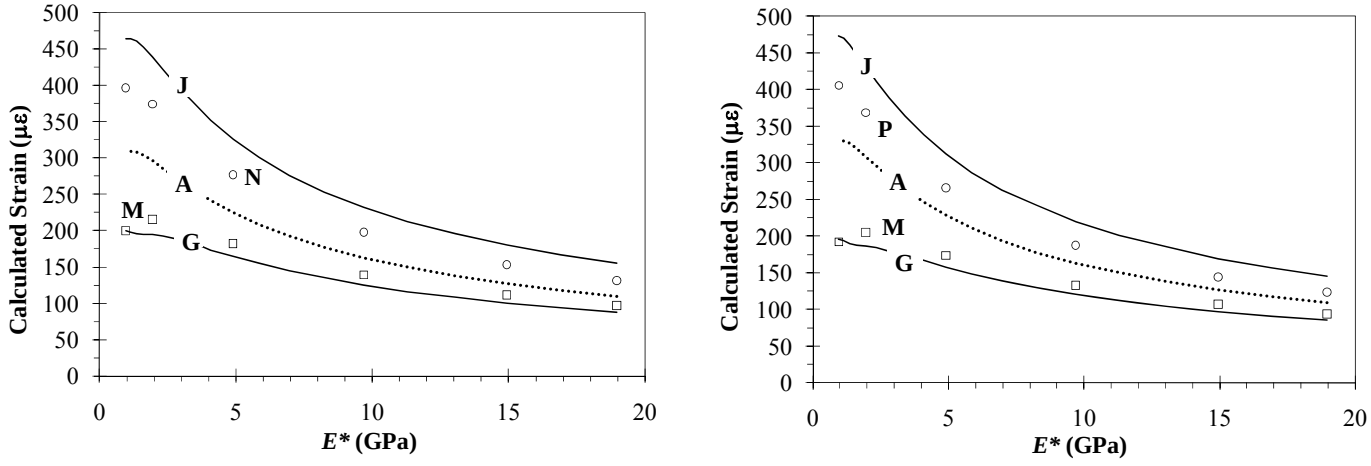

(a) Design 1 (b) Design 2

Fig. 3. Finite Element Asphalt Strain Results with Varying Material Property Variability

Table 3 provides the range of strain taken from Figs. 1 and 2 that can occur due to variability separated into cases A to F and G to L. Data was presented in this manner to show the effect of pavement material variability. Cases A to F showed 8% to 67% change in strain, while cases G to L showed 72% to 141% change in strain. Strain changes of this magnitude are significant when using instrumentation to compare products, investigate pavement performance, monitor deterioration, or to perform comparable activities since the strain changes due to variability would be greater than or equal to the anticipated strain changes being studied in many situations. Without numerous repeat measurements, this level of variability makes the use of asphalt strain gauges in thin pavements questionable for many applications.

Fig. 3 plots the effect of 15% and 30% pavement material variability on asphalt strain alongside case A as a reference. The change in strain was reduced from 72-141% at 30% pavement material variability to 32-109% at 15% pavement material variability. Behaviors were similar for designs 1 and 2.

The amount of damage occurring as a result of variability can be more meaningful than the absolute strain response. The damage was calculated using the *Asphalt Institute* transfer function [22] with constants tailored to thin pavements using the modified equation provided by Howard and Warren [23] that is shown in Eq. (3). The transfer function reduces fatigue life as strain or modulus increases. The fatigue damage per 1,000 passes (D_f) was calculated according to Miner's Law, as shown in Eq. (4).

$$N_f = 0.0138\varepsilon_t^{-3.291}\left|E^*\right|^{-0.854} \quad (3)$$

$$D_d = \left(1000 / N_d\right)*100 \quad (4)$$

N_f is the number of repetitions to fatigue cracking, ε_t is the tensile strain in the horizontal direction at the bottom of the asphalt mat (mm/mm), and E^* is the asphalt concrete dynamic modulus (psi).

Table 3 provides asphalt strain damage test results. Cases A to F represent percent change for D_f values from 0.05% to 0.74%, while cases G to L represent percent change for D_f values from 0.45% to 2.72%. The relationship of strain to damage is non-linear. In terms of damage, the effect of variability is even more apparent. Variability that can and does occur during the construction of thin flexible pavements is substantial and more formidable than it would appear in the absence of numerical analysis. Quantification of the effect of a variable on pavement performance using asphalt strain gauges is extremely difficult in thin pavements due to the large performance differences that tolerable construction variability produces.

As an example, The *Low Volume Roads* portion of *NCHRP 1-37A* suggests using 50,000 heavy vehicles as the practical minimum traffic level during a performance period. Heavy vehicles were modeled in this paper. The worst condition in Table 3 has a minimum D_f of 0.20% and a maximum D_f of 2.92%. The maximum D_f of the worst condition would exceed the 100% allowed damage after 35,000 passes, whereas the minimum D_f of the best condition would exceed the allowed damage after 500,000 passes. The best condition in Table 3 has a minimum D_f of 0.16% and a maximum D_f of 0.21%. The maximum D_f would exceed the 100% allowed damage after 475,000 passes, whereas the minimum D_f would exceed the allowed damage after 625,000 passes. For the worst case, an instrumented pavement can predict very poor performance or excellent performance depending on the variability and the extent it could be/was handled in the analysis. For the best case, the instrumented pavement would show moderate performance differences as a result of variability.

Subgrade Stress Calculation Results

Results of the FEA simulations for vertical subgrade stress in the subgrade with 0% and 30% pavement material are plotted in Figs. 4 and 5 versus the anticipated asphalt modulus. Fig. 4 shows the highest pressure occurring in the thinnest pavement over the highest M_r and the lowest pressure occurring in the thickest pavement over the lowest M_r. The behavior in both cases is intuitive. Thickness was more significant than modulus for Design 1, where the base layer was much thicker than Design 2. The base layer thickness varied 28% from the designed thickness for Design 1, which would contribute to layer thickness being more significant.

Fig. 5 shows the highest pressure occurring in pavement sections with the thinnest asphalt layer, intermediate thickness base layers, and the highest M_r. The lowest pressure occurred in the pavement with the thickest asphalt layer, thickest base layer, and lowest M_r. Design 2 had a base thickness variability equal to 18% of the base design thickness, which is considerably less than Design 1 (Fig. 4). The minimum base thickness was only 1.1 cm less than the *as designed* case, with the minimum *as built* asphalt thickness being 0.5 cm greater than the *as designed* thickness. Thus it is logical that the *as designed* layer thicknesses (case H) produce the highest stress.

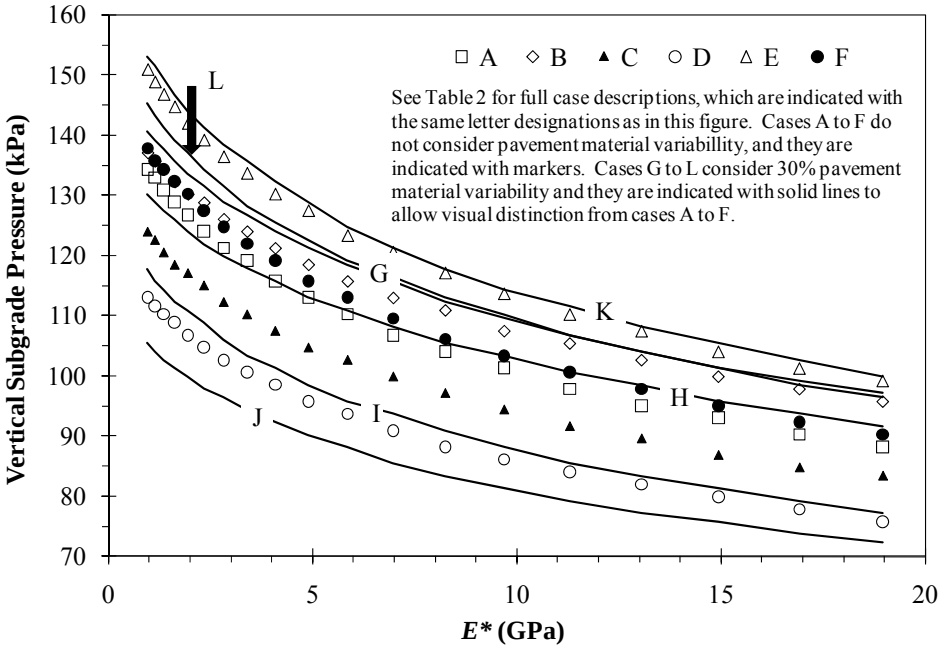

Fig. 4. Finite Element Analysis Results for Design 1 Subgrade Pressure

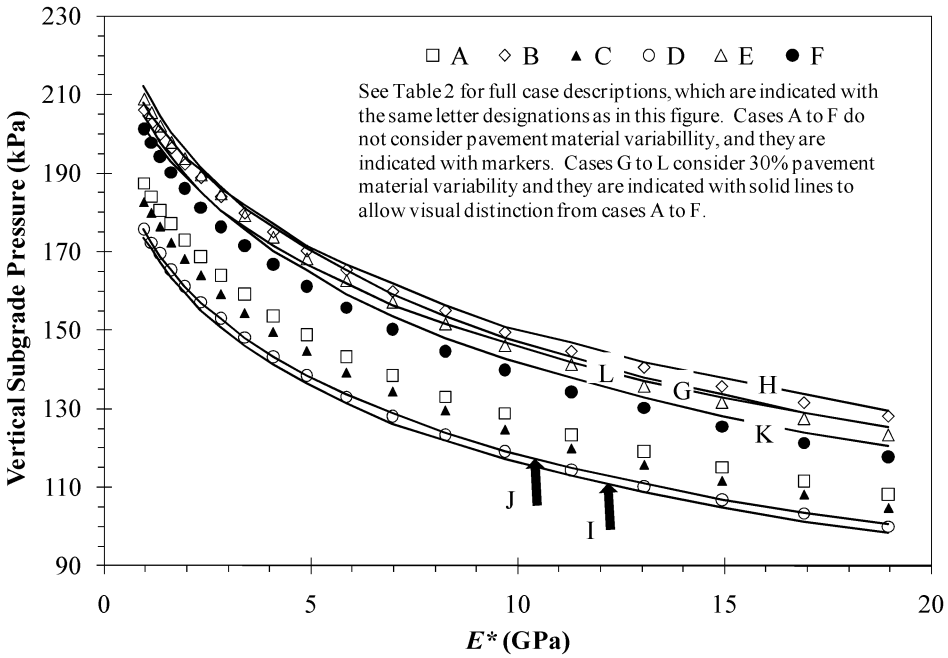

Fig. 5. Finite Element Analysis Results for Design 2 Subgrade Pressure

If one were to combine the *as designed* asphalt thickness with the minimum *as built* base thickness and the highest M_r, subgrade pressure would exceed the data shown. For variability assessment, this combination was of no interest as it did not occur. The distribution of M_r values were smaller in Design 2 than in Design 1, which also contributed to the behaviors observed for Design 2.

The amount of stress variability that can occur in a full scale pavement over a short duration is also important. Table 4 provides the range of stresses taken from Figs. 3 and 4 that can occur due to variability, separating them into cases A to F and G to L. Data presented in this manner show the effect of pavement material variability. Cases A to F show a 17% to 33% change in stress, while cases G to L show a 21% to 45% percent change in stress. Stress changes of this magnitude are formidable when using instrumentation to compare products, investigate pavement performance, and monitor deterioration but are not nearly as daunting as the changes in asphalt strain reported in the previous section. This level of variability would likely require repeat measurements but could be managed for some applications. Modeling cases with 15% pavement material variability supported this position.

The amount of rutting damage occurring as a result of variability was calculated using the *Asphalt Institute* transfer function [22], shown in Eq. (5) with calibration using data provided in [19] and [23]. The rutting damage per 1,000 passes (D_d) was calculated according to Miner's Law, as shown in Eq. (6).

$$N_d = 1.365(10^{-9})\left(\frac{0.66\sigma_d}{M_r}\right)^{-4.477} \quad (5)$$

$$D_d = (1000 / N_d) * 100 \quad (6)$$

N_d is the number of repetitions to permanent deformation (rutting) failure, σ_d is the deviator stress on the subgrade (kPa), and M_r is the subgrade resilient modulus (kPa).

Table 4 provides subgrade stress rutting damage test results. Cases A to F had percent change for D_d values from 0.05% to 6.74%. Design 1 results had less damage in comparison to Design 2. In a similar fashion, cases G to L had D_d values from 0.11% to 11.19%. Rutting damage results are higher in magnitude than fatigue cracking but are not as problematic to address from a variability standpoint. The pavements considered are thin and thus susceptible to rutting (especially Design 2), which explains the high amount of damage per 1,000 passes. When the percentage change in D_d is viewed in the context of the maximum D_d, subgrade stress variability is much less than asphalt strain variability. The percent changes in D_f for asphalt strain were 0.05% to 0.74% and 0.45% to 2.72% for cases A to F and G to L, respectively. Comparing the 0.74% change in D_f to the corresponding maximum D_f of 1.07% (as seen in Table 3) reveals that the change in damage is approaching the total amount of damage (i.e. variability is dominating the measurement. Comparison of the 2.72% change to the corresponding maximum D_f value is even greater as the maximum value is only 2.92%. Subgrade stress damage (D_d) has a percent change that is much lower than the maximum value—6.74% compared to 24.74% and 11.19% compared to 28.25%, respectively, as shown in Table 4.

Measurement Variability Calculation Results

A sensitivity analysis was performed with the finite element software to investigate the amount of variability that could occur due to sensor installation tolerances, which were ±4 mm. During the pavement construction [2], pressure cell tolerances were checked with surveying equipment, while asphalt strain gauge tolerances were estimated to be similar to that of pressure cells during

Table 4. Subgrade Stress and Rutting Damage Test Results

Design	Cases	E^* (GPa)	Minimum			Maximum			Percent Change	
			σ_d (kPa)	N_d	D_d (%)	σ_d (kPa)	N_d	D_d (%)	D_d (%)	σ_d (%)
1	A to F	0.96	113.4	17029	5.87	150.9	17181	5.82	0.05	33
		1.94	106.8	22272	4.49	141.9	22626	4.42	0.07	33
		4.89	95.8	36233	2.76	127.5	36531	2.74	0.02	33
		9.69	86.1	58435	1.71	113.7	61009	1.64	0.07	32
		14.93	79.9	81655	1.22	104.0	90944	1.10	0.13	30
		18.96	75.8	103372	0.97	99.2	112370	0.89	0.08	31
2	A to F	0.96	175.7	5554	18.01	206.0	4042	24.74	6.74	17
		1.94	161.2	8167	12.24	192.2	5513	18.14	5.89	19
		4.89	138.5	16113	6.21	170.2	9500	10.53	4.32	23
		9.69	117.1	34159	2.93	149.5	16978	5.89	2.96	28
		14.93	104.7	56381	1.77	135.7	26193	3.82	2.04	30
		18.96	99.9	69564	1.44	128.2	33786	2.96	1.52	28
1	G to L	0.96	105.4	23628	4.23	153.0	16150	6.19	1.96	45
		1.94	99.9	30035	3.33	144.0	21186	4.72	1.39	44
		4.89	90.3	47214	2.12	127.5	36531	2.74	0.62	41
		9.69	81.3	75545	1.32	113.7	61009	1.64	0.32	40
		14.93	75.8	103372	0.97	105.4	85659	1.17	0.20	39
		18.96	72.3	127738	0.78	99.2	112370	0.89	0.11	37
2	G to L	0.96	173.6	5861	17.06	212.2	3539	28.25	11.19	22
		1.94	159.8	8492	11.78	193.6	5337	18.74	6.96	21
		4.89	136.4	17253	5.80	170.2	9500	10.53	4.73	25
		9.69	117.1	34159	2.93	149.5	16978	5.89	2.96	28
		14.93	104.7	56381	1.77	137.8	24453	4.09	2.32	32
		18.96	98.5	74101	1.35	128.2	33786	2.96	1.61	30

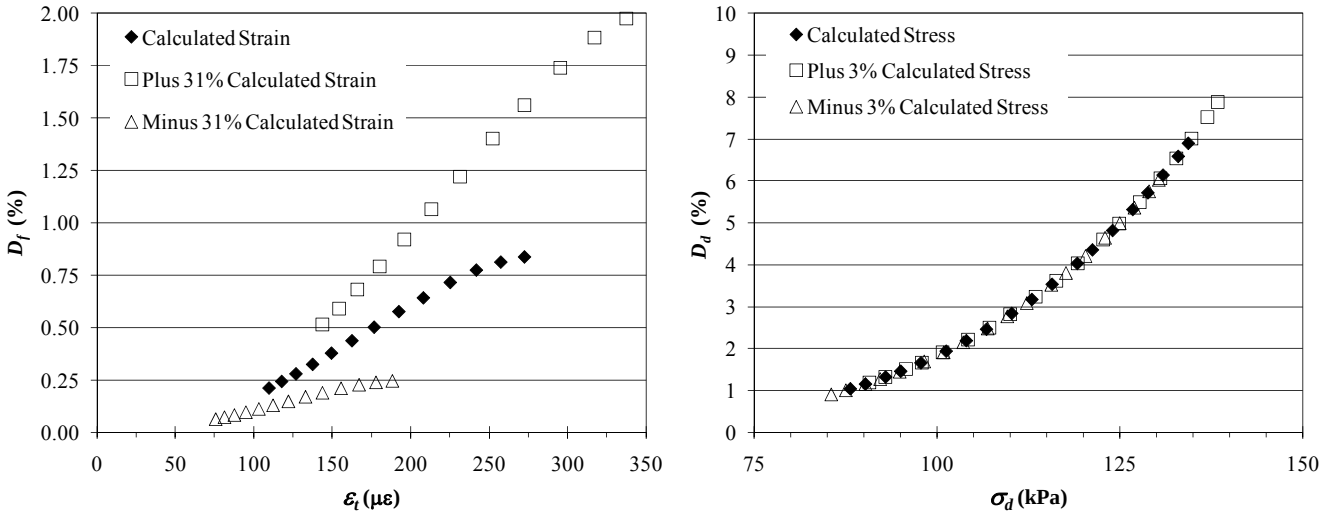

(a) Asphalt Strain (b) Subgrade Stress

Fig. 6. Effect of Sensor Positioning on Case A

construction by estimating the range of possible thicknesses of the 4.75 mm asphalt placed below the gauges. The result was a ±31% difference in asphalt strain and a ±3% difference in subgrade stress. Thin layer asphalt strains were highly sensitive to vertical position. It is noteworthy that vertical sensor position is nearly impossible to control to more than ±4 mm when installing sensors in the field directly in front of a paving train.`

Strain changes of this magnitude due to sensor positioning are significant. As an example, Fig. 6a calculates the damage of case A using the calculated strain in addition to ±31% of the calculated strain. The figure clearly illustrates the significance that small sensor position differences can have on performance. An additional 31% strain can more than double the damage per 1,000 passes relative to the expected case, while removing 31% strain can reduce the damage per 1,000 passes by more than half.

Stress changes due to sensor positioning were noteworthy but not terribly significant. As an example, Fig. 6b calculates the damage of case A using the calculated stress and ±3% of the calculated stress.

Adding 3% stress increased damage per 1,000 passes by up to 15%, while subtracting 3% stress reduced damage per 1,000 passes by up to 15%. This variability level can be handled effectively.

Summary and Conclusions

The variability of thin flexible pavements was investigated in this paper. The results show the significance of variability for a pavement built to acceptable standards. Without methods to account for variability, instrumented measurements can be misleading in some instances. Realizing that variability is present is far removed from accounting for it effectively, and this paper provides quantifiable information that can be used to account for variability either when planning for or analyzing the results of an instrumented pavement. Quantifiable data related to the variability of thin instrumented pavements was not found in literature.

Asphalt strain was shown to vary considerably due to variations in E^* and thickness, though more due to E^* than to thickness. Strain changes from 8% to 141% were calculated due to the effects of variability. Vertical sensor position shows asphalt strain can vary $\pm$31% due to sensor positioning within installation tolerances. Strain changes due to installation tolerances were shown to more than double the rate of predicted damage when the strain was increased and were shown to reduce the rate of damage by more than half when the strain was decreased. A key finding of this paper was that the use of asphalt strain gauges in thin pavements is highly prone to error and that variability can easily dominate the measurement. Without considerable measurement repetition, asphalt strain gauge readings would be difficult to use for direct comparison between test sections of an instrumented pavement.

Subgrade stress was less susceptible to variability than asphalt strain. Stress changes from 17% to 45% were calculated due to the effects of variability. Vertical sensor position shows subgrade stress can vary $\pm$3% due to sensor positioning within installation tolerances. Rutting damage due to sensor positioning was found to be much more manageable than the variability of asphalt strain, as the damage change resulting from the pressure change was in the order of 15%. Subgrade stress variability, though, was too high to neglect in any type of analysis where comparisons between measurements are to be made.

Acknowledgements

The authors would like to thank the Arkansas Highway and Transportation Department and MIRAFI Construction Products for their financial support.

References

1. Timm, D.H., Priest, A.L., and McEwen, T.V. (2004). Design and Instrumentation of the Structural Pavement Experiment at the NCAT Test Track, *NCAT Report 04-01*, National Center for Asphalt Technology, Auburn, AL, USA.
2. Warren, K.A and Howard, I.L. (2007). Sensor Selection, Installation, and Survivability in a Geosynthetic-Reinforced Flexible Pavement, *Geosynthetics International,* 14(5), pp. 298-315.
3. Baker, H.B., Buth, M.R., and Van Deusen, D.A. (1994). Minnesota Road Research Project: Load Response Instrumentation Installation and Testing Procedures, *Report MN/PR-94/01*, Minnesota Department of Transportation, Maplewood, MN, USA.
4. Sargand, S. (1994). Development of an Instrumentation Plan for the Ohio SPS Test Pavement (DEL- 23-7.48), *FHWA/OH-94/019*, FHWA, U.S. Department of Transportation, Washington DC, USA.
5. Tabatabaee, N., Al-Qadi, I.L, and Sebaaly, P.E. (1992). Field Evaluation of Pavement Instrumentation Methods, *Journal of Testing and Evaluation,* 20(2), pp. 144-151.
6. Brandon, T.L., Al-Qadi, I.L., Lacina, B.A., and Bhutta, S.A. (1996). Construction and Instrumentation of Geosynthetically Stabilized Secondary Road Test Sections, *Transportation Research Record,* No. 1534, pp. 50-57.
7. MDOT (2004). *Mississippi Standard Specifications for Road and Bridge Construction,* Mississippi Department of Transportation, Jackson, MS, USA.
8. Prowell, R.B. (2001). As-Built Properties of Experimental Sections on the 2000 NCAT Pavement Test Track, *NCAT Rep 01-02*, National Center for Asphalt Technology, Auburn, AL, USA.
9. Darter, M.I., Hudson, W.R., and Brown, J.L. (1973). Statistical Variations of Flexible Pavement Properties and Their Consideration in Design, *Proc of the Association of Asphalt Paving Technologists,* 42, pp. 589-615, Houston, TX, USA.
10. AASHTO (1985). *Proposed AASHTO Guide for Design of Pavement Structures,* NCHRP Project 20–7/24, American Association of State Highway and Transportation Officials, Washington, DC, USA.
11. Freeman, R.B. and Grogan, W.P. (1997). Statistical Analysis and Variability of Pavement Materials, *Technical Report GL – 97 – 12*, US Army Corps of Engineers Waterways Experiment Station, Vicksburg, MS, USA.
12. Brown, S.F. (1977). State-of-the-Art Report on Field Instrumentation for Pavement Experiments, *Transportation Research Record,* No. 640, pp. 13-28.
13. Siddharthan, R.V., Sebaaly, P.E., El-Desouky, M., Strand, D., and Huft, D. (2005). Heavy Off-Road Vehicle Tire-Pavement Interactions and Response, *Journal of Transportation Engineering,* 131(3), pp. 239-247.
14. Willis, J.R. and Timm, D.H. (2008). Repeatability of Asphalt Strain Measurements under Full Scale Dynamic Loading, *Transportation Research Board 87th Annual Meeting* (CD-ROM), Paper 08-2339, Washington, DC, USA.
15. Zafar, R., Nassar, W., and Elbella, A. (2005). Interaction between Pavement Instrumentation and Hot-Mix-Asphalt in Flexible Pavements, *Emirates Journal for Engineering Research,* 10(1), pp. 49-55.
16. Jorenby, B.N. and Hicks, R.G. (1986). Base Course Contamination Limits, *Transportation Research Record,* No. 1095, pp. 86-101.
17. Brunton, J.M. and Akroyde, P.M. (1990). Monitoring the Performance of a Full Scale Experimental Pavement, *Proc. of the Third International Conference on Bearing Capacity of Roads and Airfields,* pp. 585-594, Trondheim, Norway.

18. Hall, K.D. and Elliott, R.P. (1992). ROADHOG-A Flexible Pavement Overlay Design Procedure, *Transportation Research Record,* No. 1374, pp. 9-18.
19. Howard, I.L. and Warren, K.A. (2009). Finite Element Modeling of Instrumented Flexible Pavements under Stationary Transient Loading, *Journal of Transportation Engineering*, 135(2), pp. 53-61.
20. Brinkgreve, R.B.J., Broere, W., and Waterman, D. (2006). *PLAXIS 2D-Version 8 User Manual*, Plaxis bv, AN DELFT, Netherlands.
21. Huang, Y.H. (2004) *Pavement Analysis and Design,* 2nd Ed, Pearson Prentice Hall Inc., Upper Saddle River, NJ, USA.
22. AI (1982). Research and Development of the Asphalt Institutes Thickness Design Manual (MS-1), 9th Ed., *Research Report 82-2*, Asphalt Institute, Lexington, KY, USA.
23. Howard, I.L. and Warren, K.A. (2008). Performance Analysis of Heavily Instrumented Flexible Pavement, *Proceedings of Geo Congress 2008,* pp. 348-355, ASCE, New Orleans, LA, USA.